**AFRL-AFOSR-VA-TR-2018-0370**

---

# A Combined Experimental and Theoretical Study on the Hydrocarbon Decomposition

Ralf Kaiser
UNIVERSITY OF HAWAII SYSTEMS HONOLULU

---

05/09/2018
Final Report

Air Force Research Laboratory
AF Office Of Scientific Research (AFOSR)/ RTA1
Arlington, Virginia 22203
Air Force Materiel Command

# REPORT DOCUMENTATION PAGE

*Form Approved*
*OMB No. 0704-0188*

| | | |
|---|---|---|
| **1. REPORT DATE** *(DD-MM-YYYY)*<br>04-10-2018 | **2. REPORT TYPE**<br>Final Performance | **3. DATES COVERED** *(From - To)*<br>15 Oct 2014 to 14 Oct 2017 |

**4. TITLE AND SUBTITLE**
A Combined Experimental and Theoretical Study on the Unimolecular Decomposition of Hydrocarbon Surrogates Relevant to JP-8 Jet Fuel

**5a. CONTRACT NUMBER**

**5b. GRANT NUMBER**
FA9550-15-1-0011

**5c. PROGRAM ELEMENT NUMBER**
61102F

**6. AUTHOR(S)**
Ralf Kaiser

**5d. PROJECT NUMBER**

**5e. TASK NUMBER**

**5f. WORK UNIT NUMBER**

**7. PERFORMING ORGANIZATION NAME(S) AND ADDRESS(ES)**
UNIVERSITY OF HAWAII SYSTEMS HONOLULU
2530 DOLE STREET SAK D-200
HONOLULU, HI 96822-2309 US

**8. PERFORMING ORGANIZATION REPORT NUMBER**

**9. SPONSORING/MONITORING AGENCY NAME(S) AND ADDRESS(ES)**
AF Office of Scientific Research
875 N. Randolph St. Room 3112
Arlington, VA 22203

**10. SPONSOR/MONITOR'S ACRONYM(S)**
AFRL/AFOSR RTA1

**11. SPONSOR/MONITOR'S REPORT NUMBER(S)**
AFRL-AFOSR-VA-TR-2018-0370

**12. DISTRIBUTION/AVAILABILITY STATEMENT**
A DISTRIBUTION UNLIMITED: PB Public Release

**13. SUPPLEMENTARY NOTES**

**14. ABSTRACT**

The primary objectives of this project were to explore experimentally and theoretically the decomposition of prototype hydrocarbon surrogates relevant to the combustion of JP-8 and JP-10 jet fuel. This endeavor presents a major challenge as no study has been conducted to date,in which the decomposition mechanisms of these surrogates and the overall spectrum of newly formed open and closed shell molecules have been explored on line and in situ under combustion relevant conditions over a broad range of parameters (pressure, temperature). By conducting molecular beam experiments and combining these studies with electronic structure calculations, we extract information on the products, their branching ratios, the kinetics, and reaction mechanisms involved in the decomposition of JP-8 and JP-10 surrogates over a broad range of combustion relevant temperatures and pressures. These data are superior compared to those obtained from shock tube experiments (versatile detection system, complete detection of all products including radicals and thermally unstable products, branching ratios) and are very much required by the combustion community to unravel the initial processes, which trigger the decomposition of prototype hydrocarbon molecules and

**15. SUBJECT TERMS**
combustion, diagnostics, molecular beam

| | | | | |
|---|---|---|---|---|
| **16. SECURITY CLASSIFICATION OF:** | | | **17. LIMITATION OF ABSTRACT** | **18. NUMBER OF** |

Standard Form 298 (Rev. 8/98)
Prescribed by ANSI Std. Z39.18

| | | | | | |
|---|---|---|---|---|---|
| **a. REPORT**<br>Unclassified | **b. ABSTRACT**<br>Unclassified | **c. THIS PAGE**<br>Unclassified | UU | **PAGES** | **19a. NAME OF RESPONSIBLE PERSON**<br>LI, CHIPING |
| | | | | | **19b. TELEPHONE NUMBER** *(Include area code)*<br>703-696-8574 |

Standard Form 298 (Rev. 8/98)
Prescribed by ANSI Std. Z39.18

# A Combined Experimental and Theoretical Study on the Unimolecular Decomposition of Hydrocarbon Surrogates Relevant to JP-8 and JP-10 Jet Fuel

Final Report (10/15/14 – 10/14/17)

AFOSR FA9550-15-1-0011

Program Officer
Dr. Chiping Li

Ralf I. Kaiser
Principal Investigator
*Department of Chemistry*
*University of Hawaii at Manoa*
*Honolulu, HI 96822*
*ralfk@hawaii.edu*

Alexander M. Mebel
Co-Investigator
*Department of Chemistry and Biochemistry*
*Florida International University*
*Miami, FL 33199*
*mebela@fiu.edu*

## 1. Program Scope

The primary objectives of this project were to explore experimentally and theoretically the unimolecular decomposition of prototype hydrocarbon surrogates relevant to the combustion of JP-8 and JP-10 jet fuel. For JP-8, these are n-decane ($C_{10}H_{22}$) and n-dodecane ($C_{12}H_{26}$) to simulate the n-alkane fraction of JP-8. JP-10 represents principally a single-component-fuel: exo-tetrahydrodicyclopentadiene ($C_{10}H_{16}$). This endeavor presents a major challenge as no study has been conducted to date, in which the *decomposition mechanisms* of these surrogates and the *overall spectrum* of newly formed *open* and *closed shell molecules* have been explored on line and *in situ* under combustion relevant conditions over a broad range of parameters (pressure, temperature).

Our study exploited a high temperature *chemical reactor*, in which the decomposition of jet fuel surrogates can be probed systematically under combustion-like parameters (pressures between a few 100 to a few 1,000 Torr; temperatures from 500 K to 1,600 K). The nascent products are identified on line and *in situ* in a supersonic molecular beam applying versatile and highly complementary ionization techniques. These are soft electron impact ionization exploiting low energy electrons and single photon vacuum ultraviolet photoionization (VUVPI) followed by a mass spectroscopic analysis of the ions in a quadrupole mass spectrometer (QMS) and reflectron time-of-flight mass spectrometer (RETOF), respectively.

By conducting molecular beam experiments and combining these studies with electronic structure calculations, we extract information on the products, their branching ratios, the kinetics, and reaction mechanisms involved in the decomposition of JP-8 and JP-10 surrogates over a broad range of combustion relevant temperatures and pressures. These data are superior compared to those obtained from bulk shock tube experiments (versatile detection system, complete detection of *all* products including radicals and thermally unstable products, branching ratios) and are very much required by the combustion community to unravel the initial processes, which trigger the decomposition of prototype hydrocarbon molecules and ‘switch on’ the supply of radicals in the combustion of JP-8 and JP-10 jet fuel within the first few 10 μs. Those studies also elucidated the rate-controlling processes together with key reaction pathways and mechanisms in fuel decomposition processes.

## 2. Key Results

We completed the experimental and computational studies on the decomposition of two key surrogates of the aliphatic component of JP-8 [n-decane ($C_{10}H_{22}$), n-dodecane ($C_{12}H_{26}$)] up to 1,600 K (**P1**, **P2**). This was expanded to a theoretical study of the decomposition of three n-butylcyclohexane isomers (n-, i-, t- $C_{14}H_{10}$) as representatives for substituted cycloalkanes in JP-8 (**P3**). Finally, we systematically explored the unimolecular decomposition of JP-10 both experimentally and computationally (**P4**, **P5**).

### 2.1. Decane and Dodecane

Our investigations represented the very first in a series of combined experimental and theoretical studies to probe the pyrolysis and decomposition of prototype JP-8 jet fuel surrogates: *n*-decane ($C_{10}H_{22}$) (**P1**) and *n*-dodecane ($C_{12}H_{26}$) (**P2**). The pyrolysis was explored in a high temperature *chemical reactor,* in which the decomposition of jet fuel surrogates was probed systematically under combustion-like temperatures up to 1,600 K. The nascent product distribution – *including radicals and thermally labile closed-shell species* – were explored comprehensively on-line and *in situ* in a supersonic molecular beam exploiting soft photoionization (PI) with single photon VUV light followed by a mass spectroscopic analysis of the ions in a reflectron time of flight mass spectrometer (Re-TOF-MS). This study aimed to probe the *initial bond rupture processes and hence the primary reaction products* while simultaneously excluding successive (higher order) reactions of the initially formed species, which lead to molecular mass growth processes. Finally, by combining these studies with electronic structure and theoretical kinetics calculations, we extract data on the products, their branching ratios, and reaction mechanisms involved in the decomposition of JP-8 surrogates over a broad range of combustion-relevant temperatures.

Here, for the first time, the initial decomposition products of *n*-(do)decane - including radicals and thermally labile closed-shell species were probed in experiments, which effectively exclude mass growth processes. Fifteen different products were identified, such as molecular hydrogen ($H_2$), C2 to C7 1-alkenes [ethylene ($C_2H_4$) to 1-heptene ($C_7H_{14}$)], C1-C3 radicals [methyl ($CH_3$), ethyl ($C_2H_5$), allyl ($C_3H_5$)], small C1-C3 hydrocarbons [acetylene ($C_2H_2$), allene ($C_3H_4$), methyl-acetylene $C_3H_4$], as well as the reaction products [1,3-butadiene ($C_4H_6$), 2-butene ($C_4H_{10}$)] (Fig. 1). Electronic structure calculations carried out at the G3(CCSD,MP2)//B3LYP/6-311G(d,p) level of theory combined with RRKM/Master Equation calculations of rate constants for relevant reaction steps showed that, e.g., *n*-dodecane decomposes initially by a non-terminal C-C bond cleavage and producing a mixture of alkyl radicals from ethyl to decyl with approximately equal branching ratios (Figs. 2 & 3). The alkyl radicals were found to be unstable under the experimental conditions and to rapidly dissociate either directly by C-C bond $\beta$-scission to produce ethylene ($C_2H_4$) plus a smaller 1-alkyl radical with the number of carbon atoms diminished by two or via 1,5-, 1,6-, or 1,7- 1,4-, 1,9-, or 1,8-H shifts followed by C-C $\beta$-scission producing alkenes from propene to 1-nonene together with smaller 1-alkyl radicals. The stability and hence the branching ratios of higher alkenes decrease as temperature increases. The C-C $\beta$-scission continues all the way to the propyl radical ($C_3H_7$), which dissociates to methyl ($CH_3$) plus ethylene ($C_2H_4$). In addition, at higher temperatures, alternative mechanism contributes, in which hydrogen atoms abstract hydrogen from $C_{12}H_{26}$ producing various n-dodecyl radicals and these radicals then decompose by C-C bond $\beta$-scission to C3 to C11 alkenes.

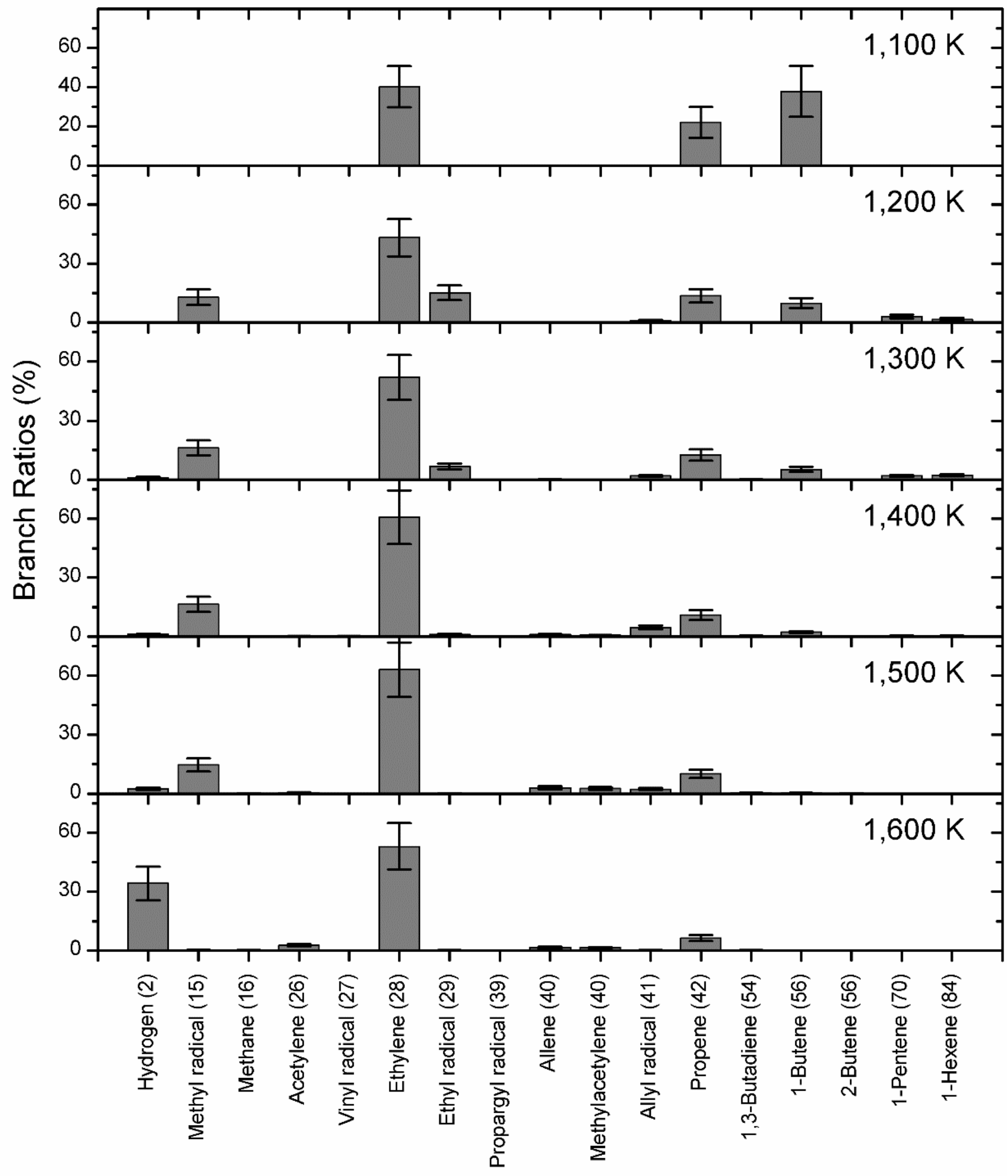

Fig. 1a: Overall branching ratios of the species detected during the decomposition of *n*-decane at temperatures from 1,100 K to 1,600 K.

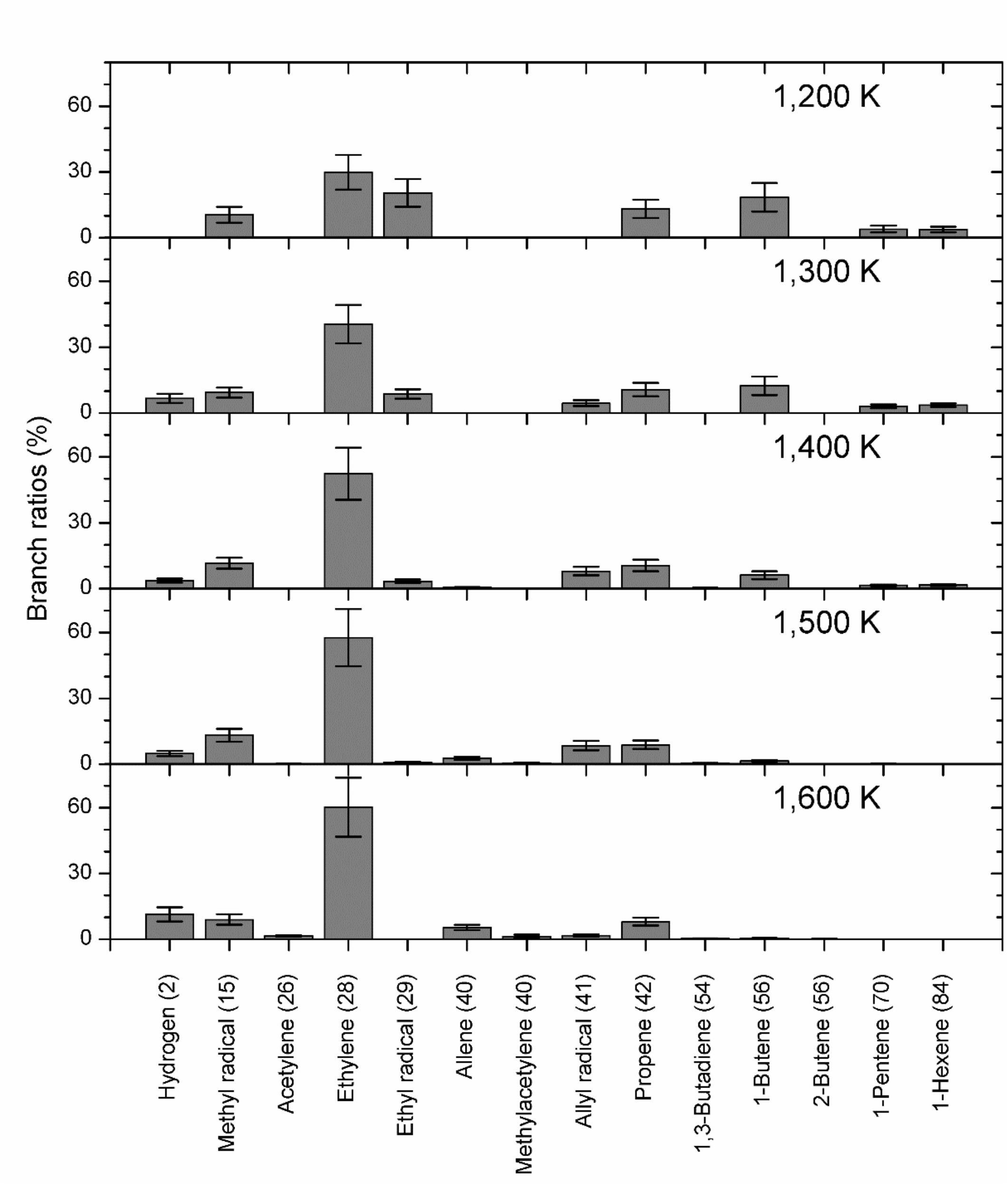

Fig. 1b: Overall branching ratios of the species detected during the decomposition of *n*-decane at temperatures from 1,200 K to 1,600 K.

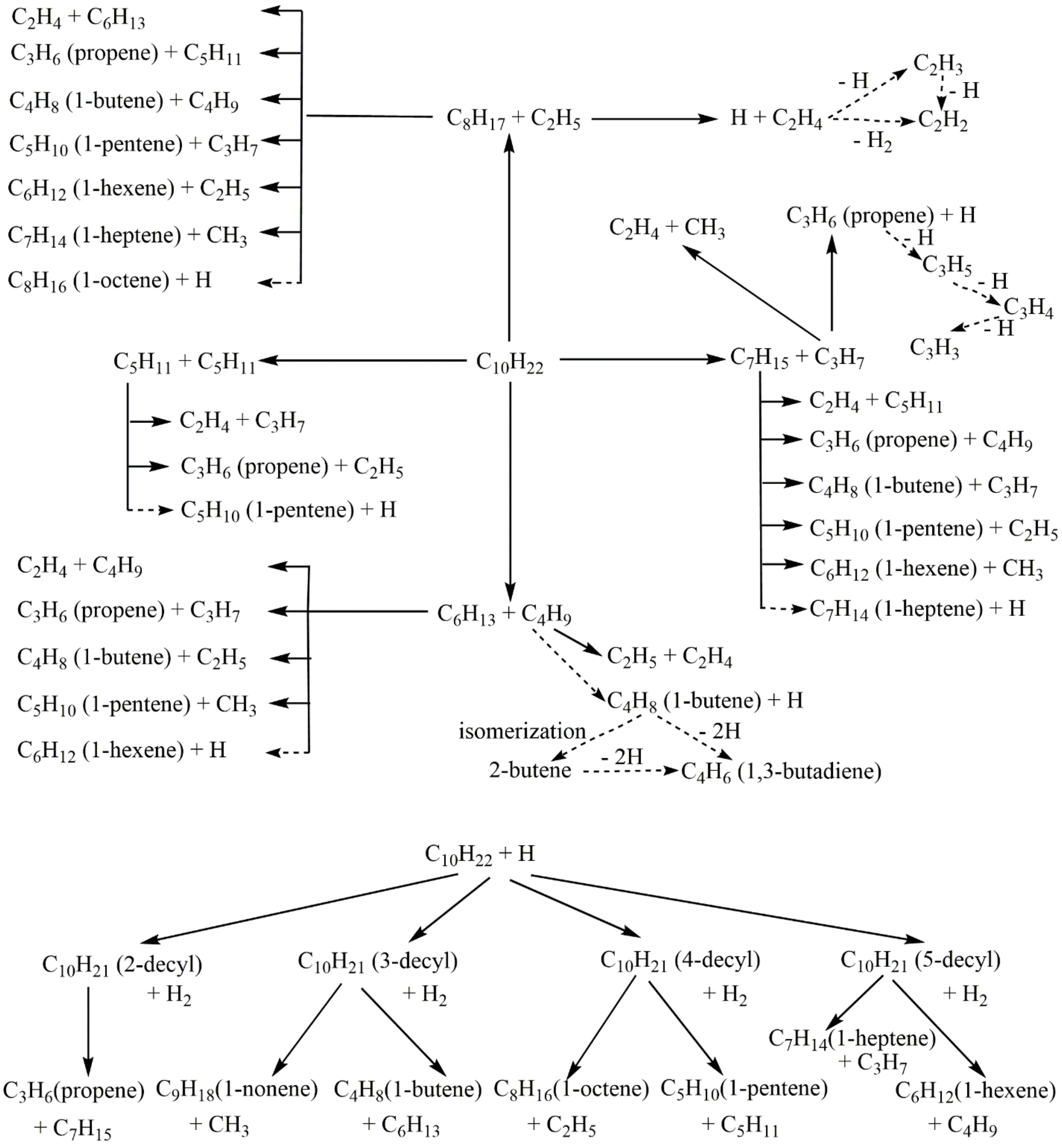

Fig. 2a: Compiled reaction mechanism for the pyrolysis of *n*-decane.

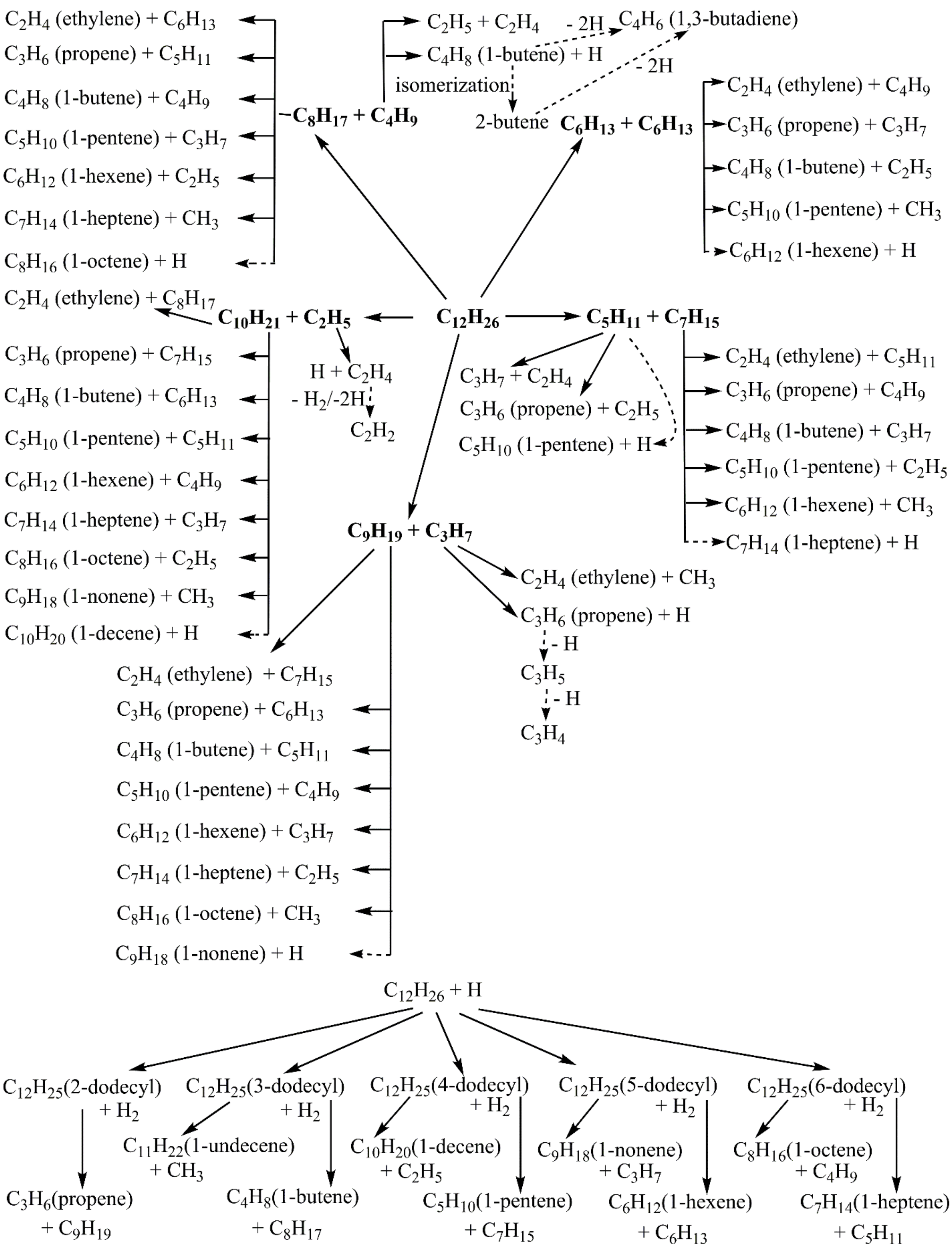

Fig. 2b Compiled reaction mechanism for the pyrolysis of *n*-dodecane.

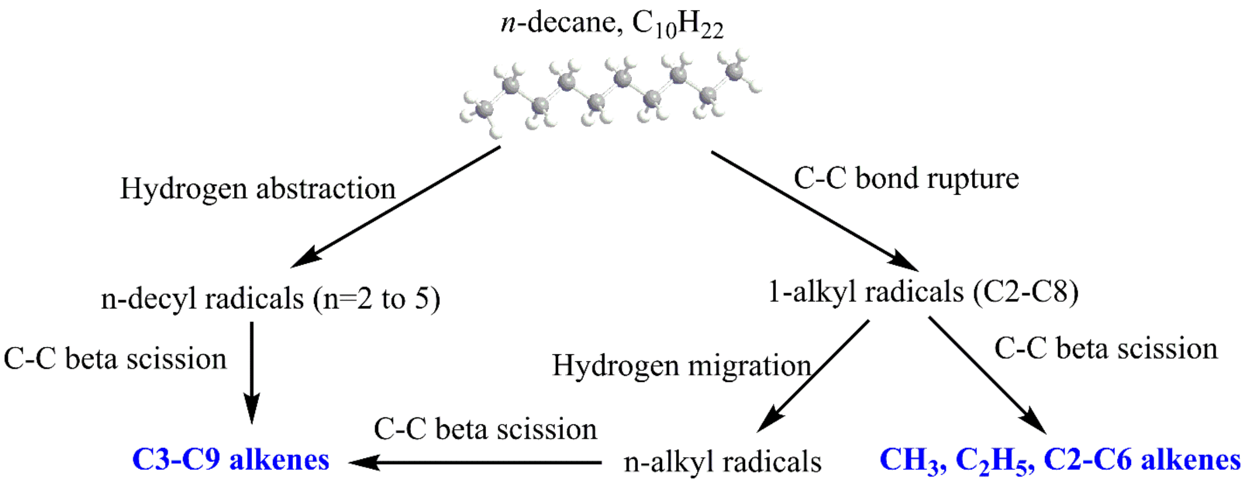

Fig. 3a: Summary of global reaction mechanisms leading to primary reaction products in the decomposition of *n*-decane.

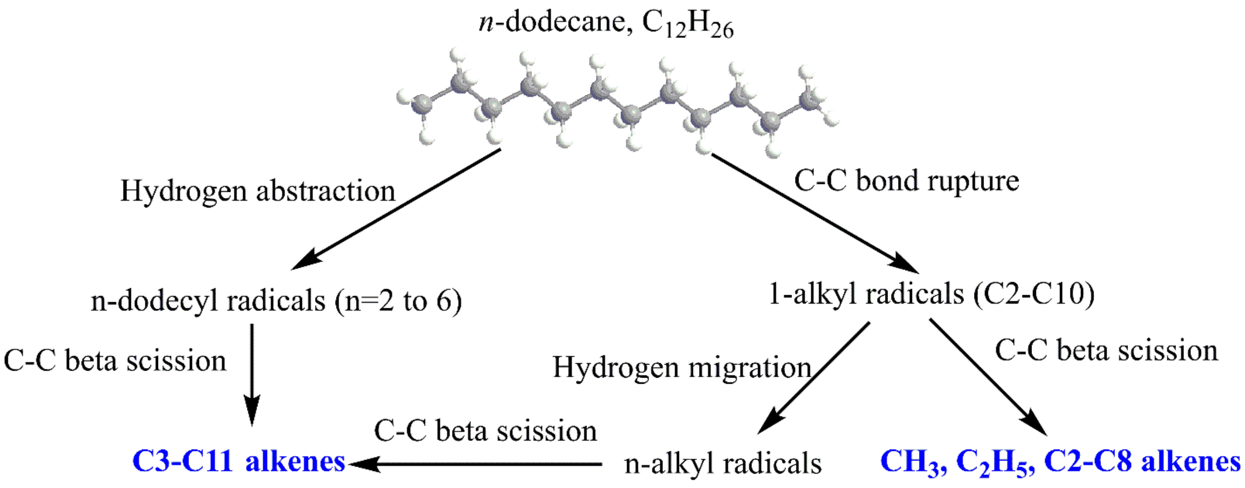

Fig. 3b: Summary of global reaction mechanisms leading to primary reaction products in the decomposition of *n*-dodecane.

## 2.2. n-, i, t-Butylcyclohexane

*Ab initio* G3(CCSD,MP2)//B3LYP/6-311G(d,p) calculations of potential energy surfaces have been carried out to unravel the mechanism of the initial stages of pyrolysis of three $C_{10}H_{14}$ isomers: *n*-, *s*-, and *t*-butylbenzenes (**P3**). The computed energetic and molecular parameters have been utilized in RRKM-Master Equation calculations to predict temperature- and pressure-dependent rate constants and product branching ratios for the primary unimolecular decomposition of these molecules and for the secondary decomposition of their radical fragments (Fig. 4). The results showed that the primary dissociation of *n*-butylbenzene produces mostly benzyl ($C_7H_7$) + propyl ($C_3H_7$) and 1-phenyl-2-ethyl ($C_6H_5C_2H_4$) + ethyl ($C_2H_5$) with their relative yields strongly dependent on temperature and pressure, together with a minor amount of 1-phenyl-prop-3-yl ($C_9H_{11}$) + methyl ($CH_3$). Secondary decomposition reactions that are anticipated to occur on a nanosecond scale under typical combustion conditions split propyl ($C_3H_7$) to ethylene ($C_2H_4$) + methyl ($CH_3$), ethyl ($C_2H_5$) to ethylene ($C_2H_4$) + hydrogen (H), 1-phenyl-2-ethyl ($C_6H_5C_2H_4$) mostly to styrene ($C_8H_8$) + hydrogen (H) and to a less extent to phenyl ($C_6H_5$) + ethylene ($C_2H_4$), and 1-phenyl-prop-3-yl ($C_9H_{11}$) predominantly to benzyl ($C_7H_7$) + ethylene ($C_2H_4$). The primary decomposition of *s*-butylbenzene is predicted to produce 1-phenyl-1-ethyl ($C_6H_5CHCH_3$) + ethyl ($C_2H_5$) and a minor amount of 1-phenyl-prop-1-yl ($C_9H_{11}$) + methyl ($CH_3$) and then, 1-phenyl-1-ethyl ($C_6H_5CHCH_3$) and 1-phenyl-prop-1-yl ($C_9H_{11}$) rapidly dissociate to styrene ($C_8H_8$) + hydrogen (H) and styrene ($C_8H_8$) + methyl ($CH_3$), respectively. *t*-Butylbenzene nearly exclusively decomposes to 2-phenyl-prop-2-yl ($C_9H_{11}$) + methyl ($CH_3$) and further, 2-phenyl-prop-2-yl ($C_9H_{11}$) rapidly eliminates a hydrogen atom to form 2-phenylpropene ($C_9H_{10}$). If hydrogen atoms or other reactive radicals are available to make a direct hydrogen atom abstraction from butylbenzenes possible, the $C_{10}H_{13}$ radicals (1-phenyl-but-1-yl, 2-phenyl-but-2-yl, *t*-phenyl-isobutyl) can be formed as the primary products from *n*-, *s*-, and *t*-butylbenzene, respectively. Secondary decomposition of 1-phenyl-but-1-yl leads to styrene ($C_8H_8$) + ethyl ($C_2H_5$), whereas 2-phenyl-but-2-yl and *t*-phenyl-isobutyl dissociate to 2-phenylpropene ($C_9H_{10}$) + methyl ($CH_3$). Thus, the three butylbenzene isomers produce distinct, but overlapping nascent pyrolysis fragments, which likely affect the successive oxidation mechanism and combustion kinetics of these JP-8 fuel components. Temperature- and pressure-dependent rate constants generated for the initial stages of pyrolysis of butylbenzenes are recommended for kinetic modeling.

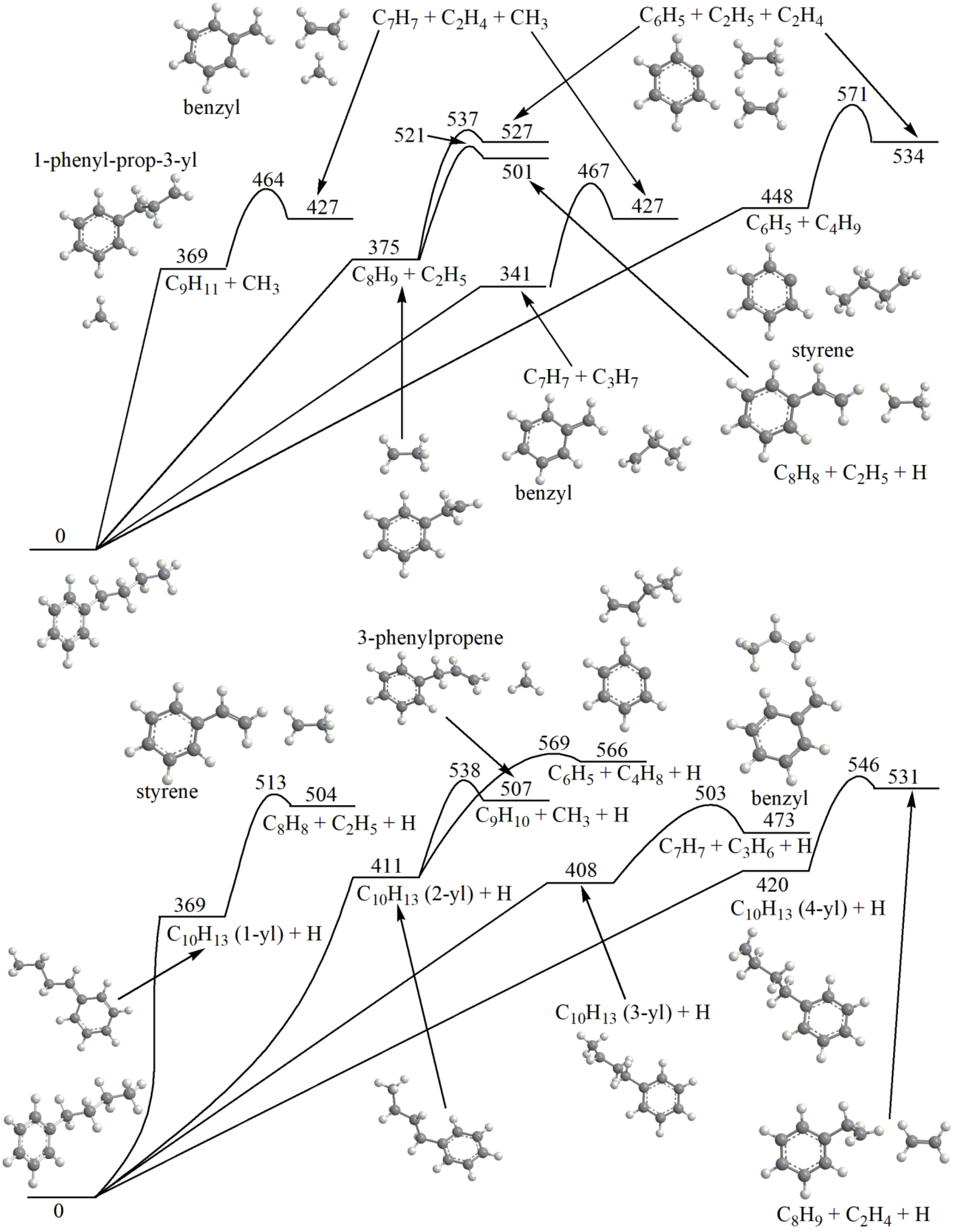

Fig. 4a: Potential energy diagram for the primary and most favorable secondary decomposition channels of *n*-butylbenzene. All relative energies with respect to the parent molecule are given in kJ mol$^{-1}$.

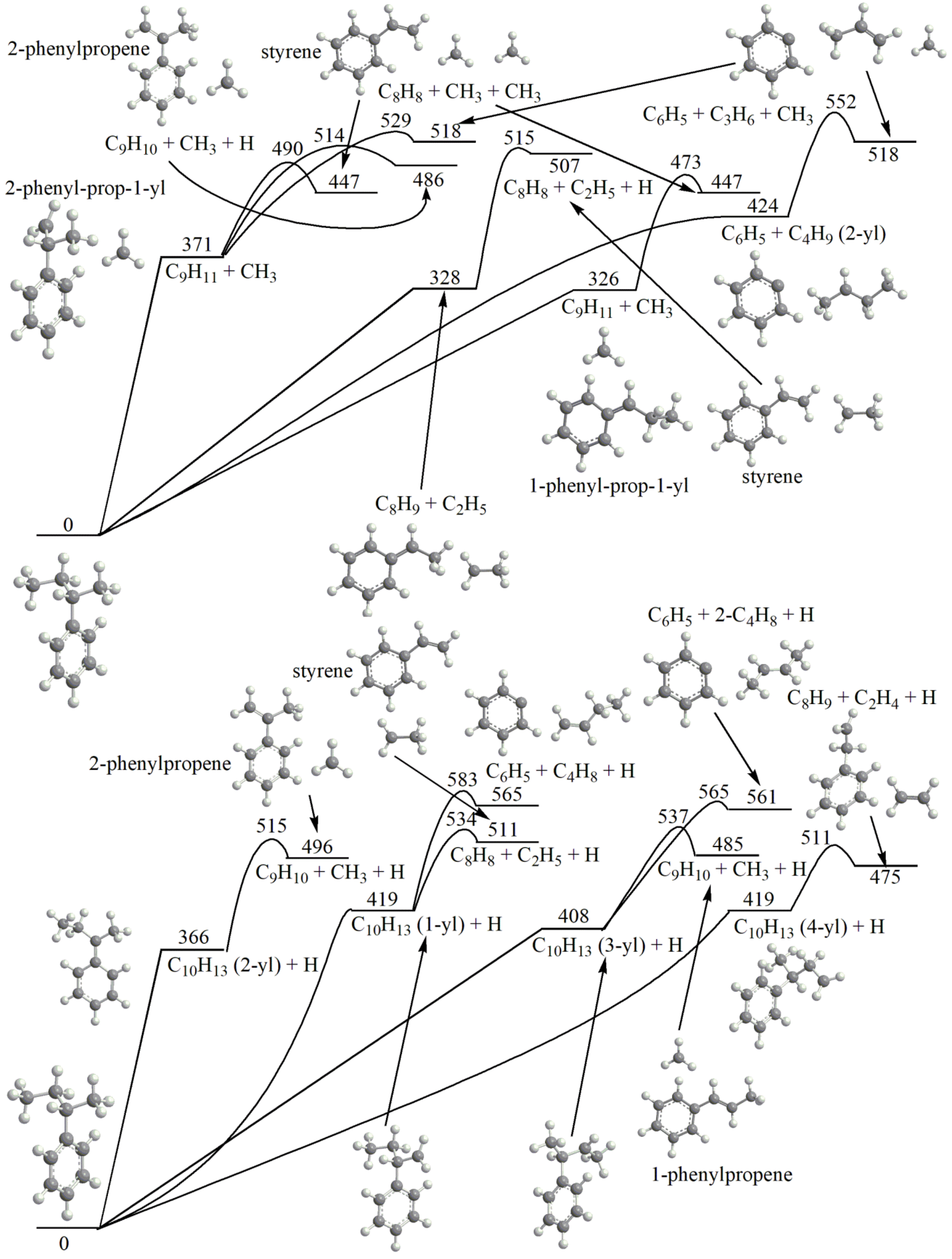

Fig. 4b: Potential energy diagram for the primary and most favorable secondary decomposition channels of *s*-butylbenzene. All relative energies with respect to the parent molecule are given in kJ mol$^{-1}$.

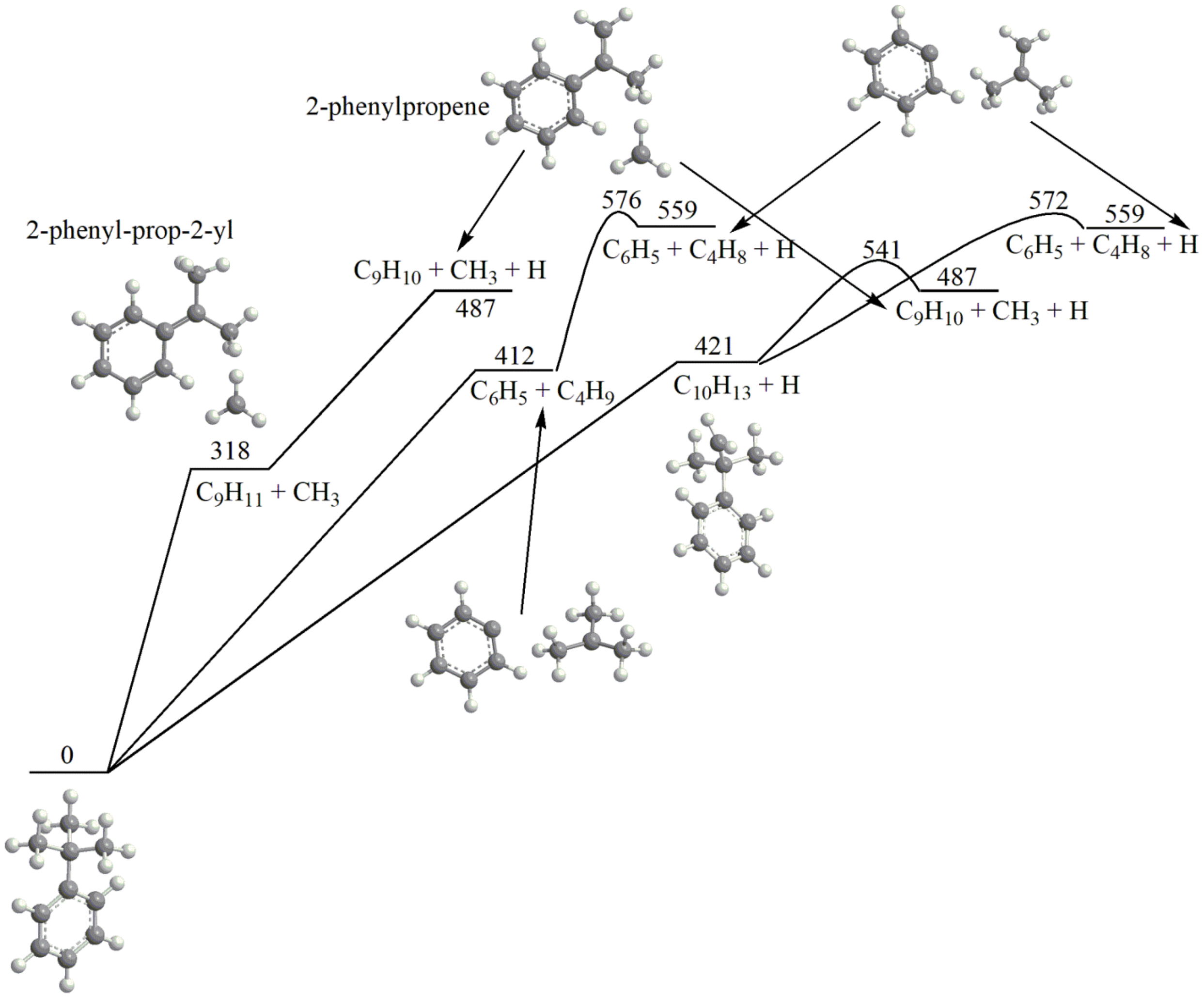

Fig. 4c: Potential energy diagram for the primary and most favorable secondary decomposition channels of *t*-butylbenzene. All relative energies with respect to the parent molecule are given in kJ mol$^{-1}$.

## 2.3. Exo-tetrahydrodicyclopentadiene

Exploiting a high temperature *chemical reactor*, the pyrolysis of JP-10 (*exo*-tetrahydrodicyclopentadiene) was explored at reactor residence times from a few tens of microseconds to typically 150 ms (**P4**). The experimental studies were supported by electronic structure calculations (**P5**). All products were identified *in situ* in supersonic molecular beams via single photon VUV photoionization coupled with mass spectroscopic detection in a ReTOF-MS. These studies were designed to probe the initial (low residence times) and also higher order reaction products (higher residence times) formed in the decomposition of JP-10 - including radicals and thermally labile closed-shell species. Altogether, 43 products were detected and quantified including C1-C4 alkenes, dienes, C3-C4 cumulenes, alkynes, eneynes, diynes, cycloalkenes, cyclo-dienes, aromatic molecules, and most important, radicals such as ethyl, allyl, and methyl produced at lower residence times (Fig. 5). At longer residence times, the predominant fragments are molecular hydrogen ($H_2$), ethylene ($C_2H_4$), propene ($C_3H_6$), cyclopentadiene ($C_5H_6$), cyclopentene ($C_5H_8$), fulvene ($C_6H_6$), and benzene ($C_6H_6$). Accompanied by electronic structure calculations, the initial JP-10 decomposition via C-H bond cleavage resulting in the formation of initially six $C_{10}H_{15}$ radicals were found to explain the formation of all products detected in both sets of experiments (Fig. 6). These radicals are not stable under the experiment conditions and further decompose via C-C bond $\beta$-scission processes. These pathways result in ring opening in the initial tricyclic carbon skeletons of JP-10. Intermediates accessed after the first $\beta$-scission can further isomerize or dissociate. Polycyclic aromatic hydrocarbons (PAHs) (naphthalene, acenaphthylene, biphenyl) are only detected at higher residence times and pressures and hence are likely formed via molecular growth processes under these conditions at elevated residence times and pressures.

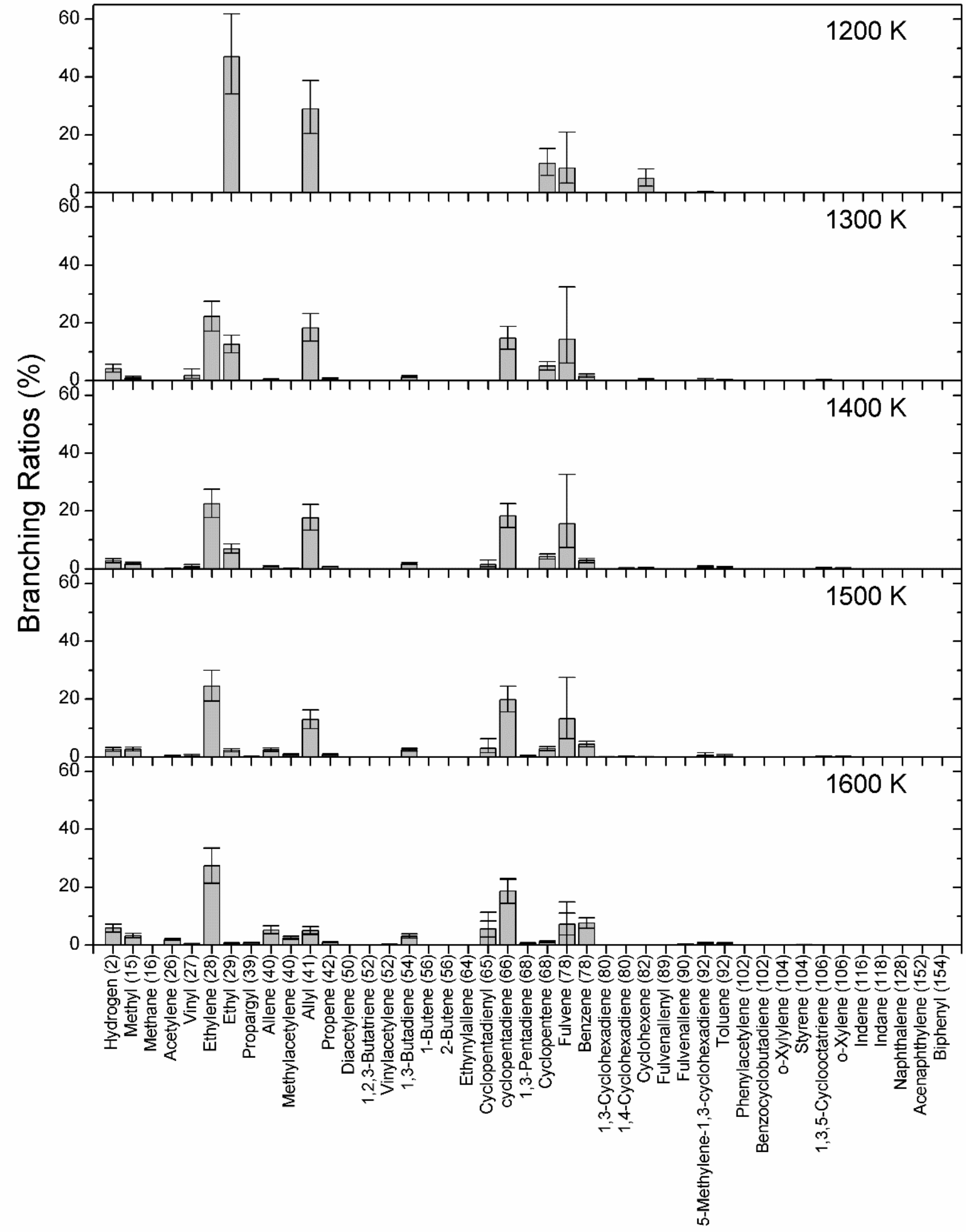

Fig. 5a: Overall branching ratios of the species obtained in the decomposition of JP-10 (ALS) in temperatures range from 1,200 to 1,600 K.

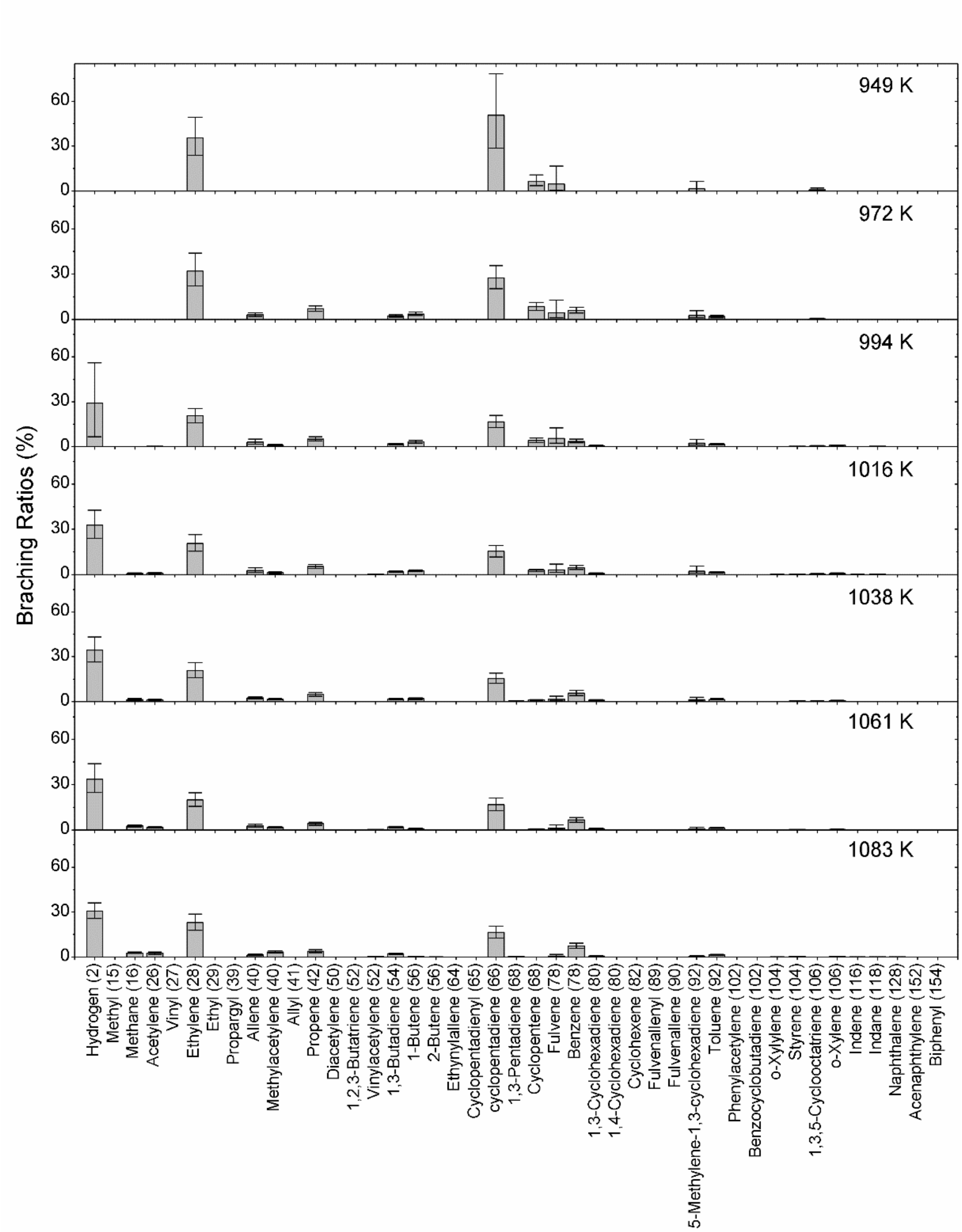

Fig. 5b: Overall branching ratios of the species obtained in the decomposition of JP-10 (NSRL) in temperatures range from 949 to 1,083 K.

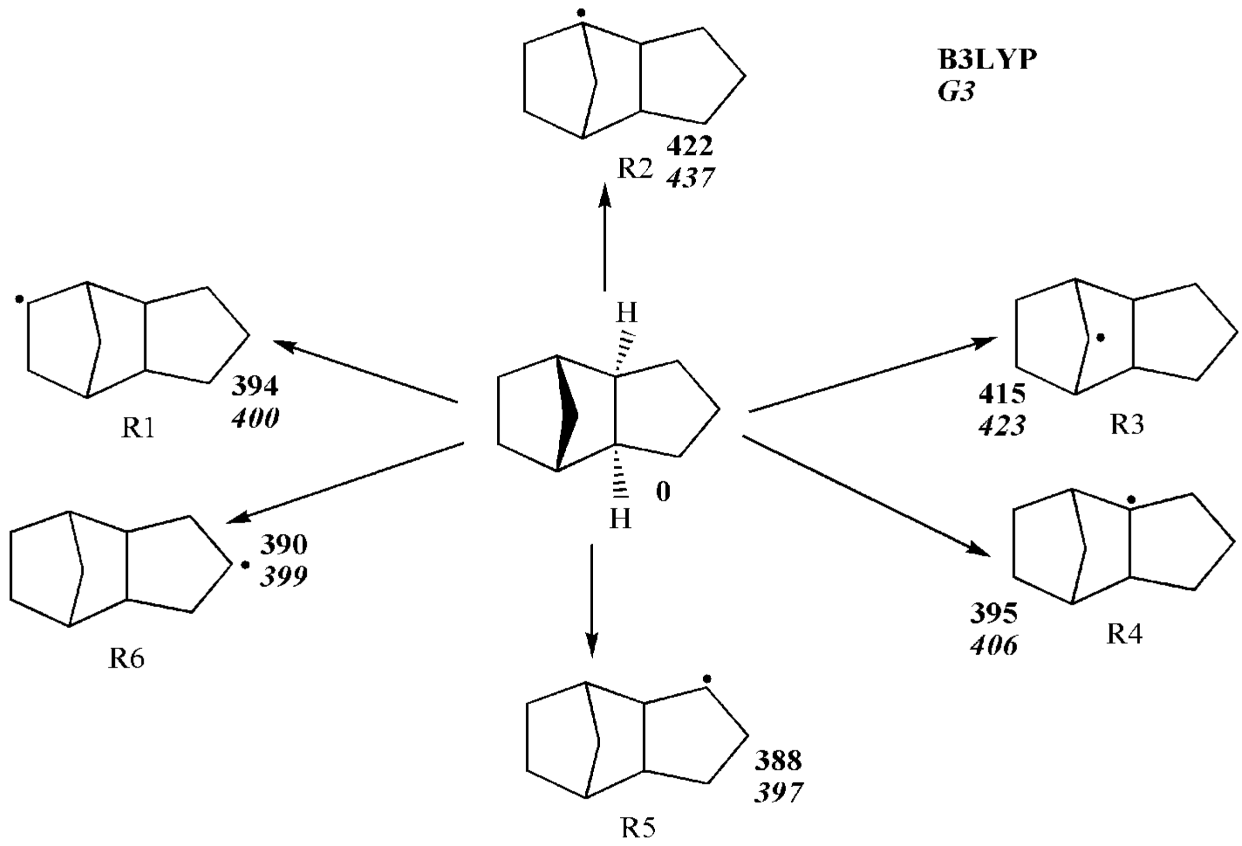

Fig. 6a: Radicals formed by initial C-H bond cleavages in JP-10. Reaction endoergicities calculated at the B3LYP/6-311G** (plain numbers) and G3 levels (italic numbers) are given in kJ mol$^{-1}$.

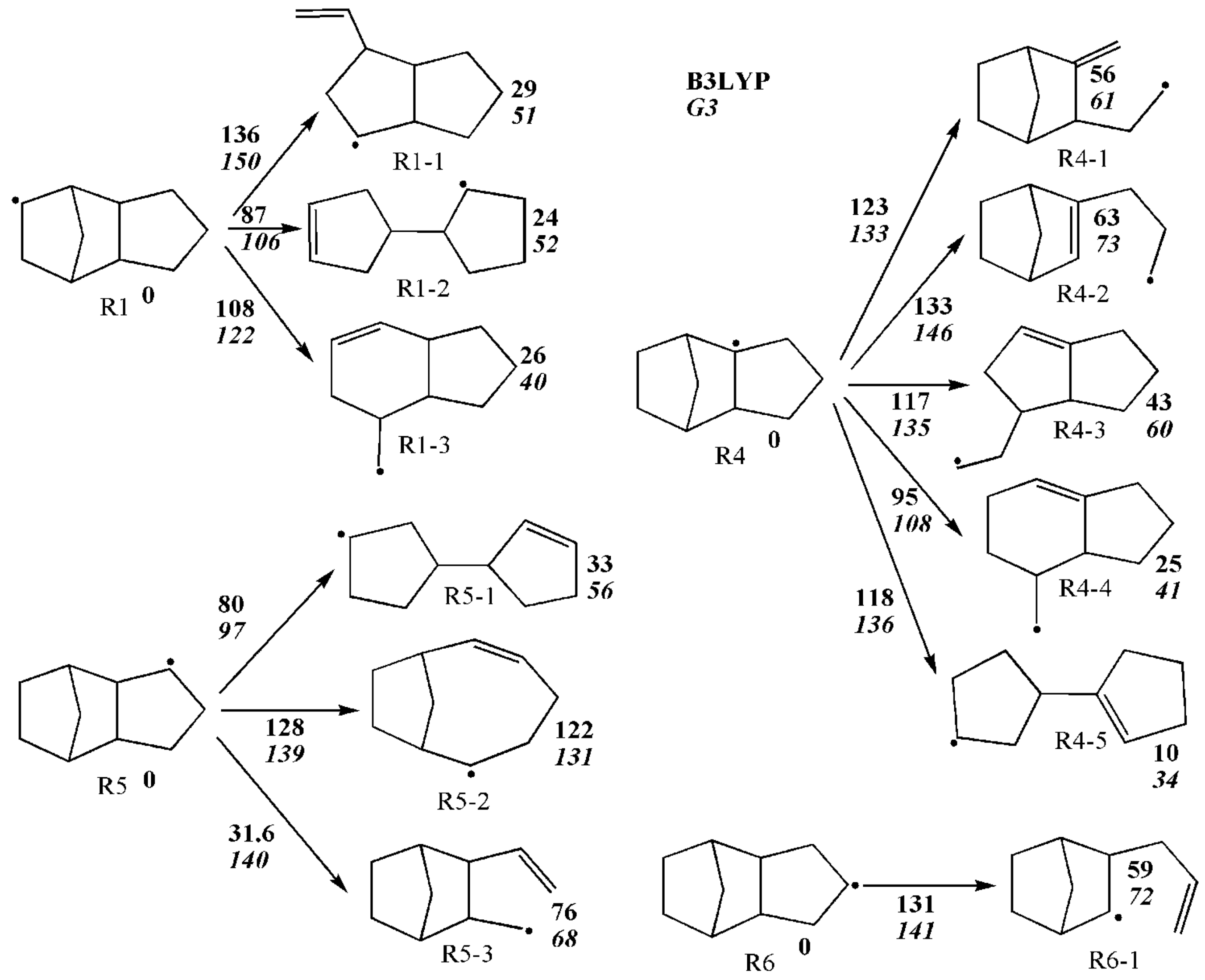

Fig. 6b: Energetics of various initial *β*-scission processes in the R1, R4, R5, and R6 radicals. Relative energies calculated at the B3LYP/6-311G** (plain numbers) and G3 levels (italic numbers) are given in kJ mol$^{-1}$.

## 3. Experimental Approch

For the aforementioned experiments, the centerpiece of the experimental studies was a resistively heated high temperature *chemical reactor* adapted from the Chen source (Fig. 7). This device allows an experimental simulation of combustion relevant conditions at temperatures up to 1,600 K and pressures up to a few 1,000 Torr. A gas mixture of the closed shell hydrocarbon with helium buffer gas is released into a resistively heated silicon carbide tube of an inner diameter of 1 mm and a length of 20 mm. The bimolecular reaction regime can be controlled by carefully adjusting the percentage composition of the hydrocarbon and the helium. Our experiments suggest that residence times between 10 μs and a few 100 μs can be achieved. The heated silicon carbide tube - the centerpiece of the chemical reactor - can be operated at temperatures up to 1,600 K by tuning the current and hence the heating power between 5 and 45 Watts.

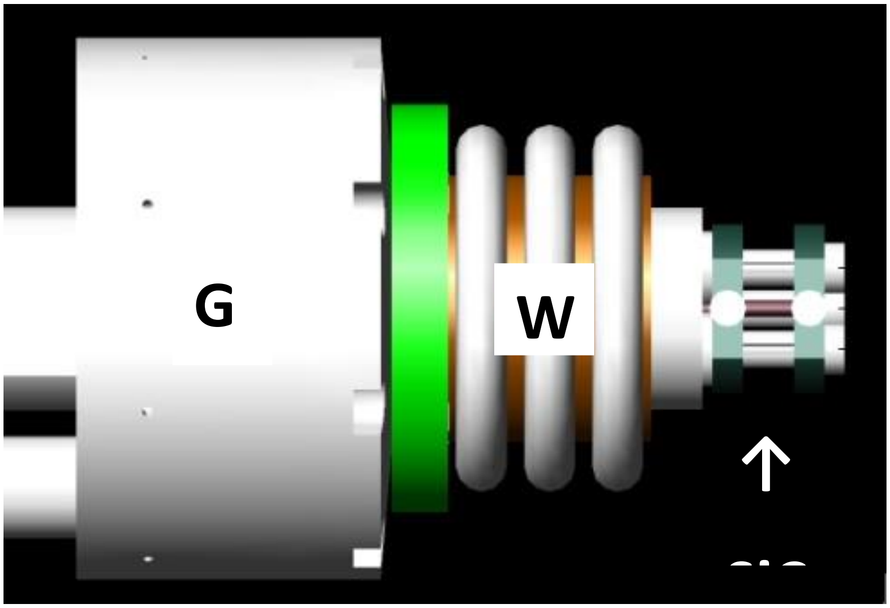

Figure 7: Schematic side view of the resistively heated *chemical reactor* consisting of the gas delivery system (G), the silicon carbide tube (SiC), and the water cooling system (W).

Which detection scheme should be incorporated to elucidate the nature of the decomposition products? Spectroscopic detection schemes like laser induced fluorescence (LIF) and Rydberg tagging (H, D, O) are restricted to species with well-established spectroscopic fingerprints such as simple di- and triatomic species like dicarbon ($C_2$), tricarbon ($C_3$), methylidyne (CH), carbene ($CH_2$).  Hence, this approach does not present a versatile detection strategy and is not suitable to investigate the thermal decomposition products. Hence *universal* and *sensitive* detection schemes are critical to monitor the products within the molecular beam on line and *in situ*. Therefore, to identify the products and to determine their pressure and temperature dependent branching ratios, the reactor was incorporated into a molecular beam machine at the Chemical Dynamics Beamline (tunable VUV soft photoionization) of the Advanced Light Source.

Here, the technique of soft, fragment free single vacuum ultraviolet (VUV) photon ionization is exploited (Fig. 8). The chemical reactor is incorporated into the molecular beam machine at the Chemical Dynamics Beamline (9.0.2.) of the Advanced Light Source; these studies are conducted in collaboration with Dr. Musahid Ahmed. In the molecular beam machine, after passing a skimmer located 10 mm downstream from the silicon carbide (SiC) nozzle, quasi continuous tunable vacuum ultraviolet (VUV) light from the Advanced Light Source crosses the neutral molecular beam at the extraction region of a Wiley–McLaren Reflectron Time-of-Flight mass spectrometer (ReTOF-MS) (Fig. 9). *Fragment–free* VUV photoionization mass spectrometry – a *soft ionization method* - is unmatched by traditional ionization techniques utilizing *hard* electron impact schemes. In most of the cases, similar to *soft* electron impact ionization, VUV photoionization only results in the formation of parent ion of the product molecule without forming fragment ions. On the other hand, the resolution of the VUV light can be enhanced practically to 0.05 eV. The ions of the photoionized molecules are then extracted and collected by a microchannel plate detector in a reflectron TOF mode utilizing a multi-channel scaler. The photoionization efficiency (PIE) curves can be obtained by plotting the relevant ion counts at a desired mass-to-charge ratio, m/z, versus the photoionization energy between 7.4 eV and 15.0 eV in steps of 0.05 eV. Based on known PIE curves of the individual isomers of a well-defined mass, the recorded PIE curves are then fit via a linear combination with known PIE curves of various isomers to extract the nature of the products formed and their branching ratios. Note that PIE curves of the isomers can be recorded in separate calibration experiments.

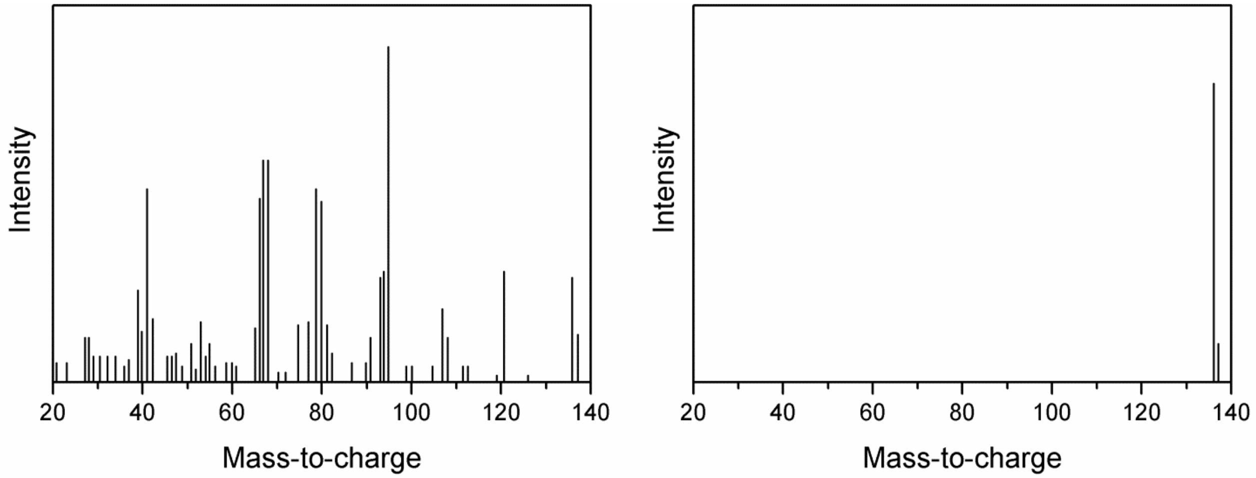

Figure 8: Mass Spectrum of *exo*-tetrahydrodicyclopentadiene obtained with hard (70 eV; left) and soft (10 eV; right) electron impact / single vacuum ultraviolet photon ionization demonstrating the unique advantage of soft photoionization techniques.

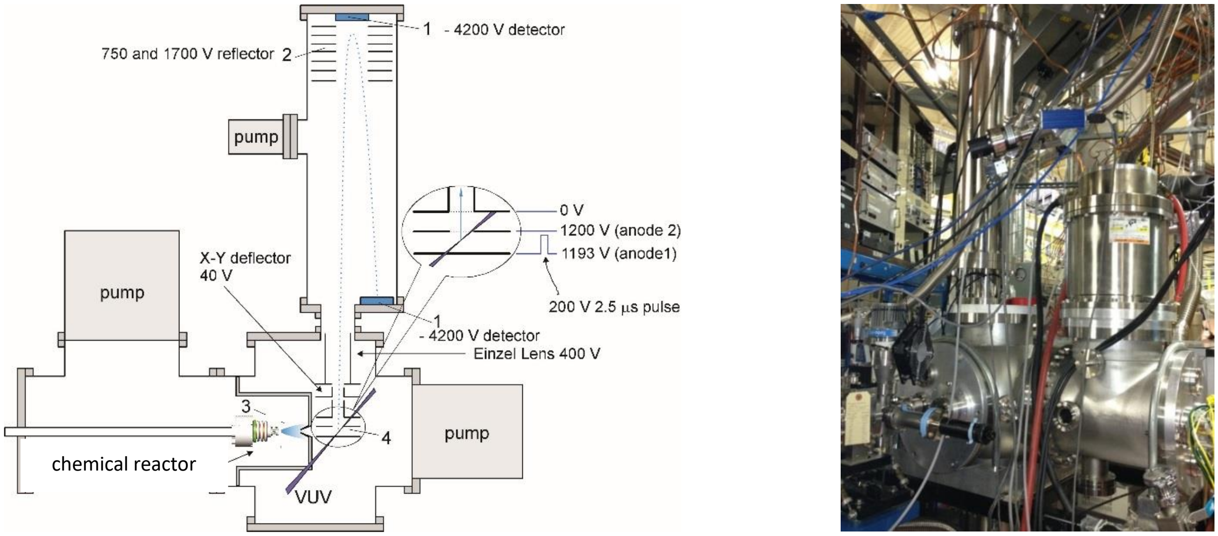

Figure 9: Schematic presentation of the incorporation of the chemical reactor in the molecular beam machine at the Chemical Dynamics Beamline together with the VUV beam path. 1) microchannel plate detectors, 2) reflector mirror, 3) molecular beam expansion, 4) ion optics.

## 4. Computational Approch

Geometries of various primary and secondary decomposition products of *n*-decane, *n*-dodecane, butylbenzene isomers, and JP-10 as well as transition states for secondary decomposition reactions (isomerizations and C-C and C-H bond $\beta$-scissions) and for direct hydrogen atom abstractions by hydrogen atoms were optimized using the density functional B3LYP method with the 6-311G(d,p) basis set. Vibrational frequencies of various local minima and transition states were computed at the same level of theory. Relative energies for all species were refined by single-point calculations at the G3(CCSD,MP2) level of theory, which included the empirical higher level correction (HLC), using B3LYP/6-311G(d,p) optimized geometries and including zero-point vibrational energy corrections (ZPE) also obtained at B3LYP/6-311G(d,p). The inclusion of the HLC increases the calculated strengths of C-H bonds by 7 kJ mol$^{-1}$, decreases relative energies of transition states and products for the hydrogen atom abstraction reactions also by 7 kJ mol$^{-1}$, is insignificant for C-C bond cleavages, and zero by definition for C-C bond $\beta$-scissions. The G3(CCSD,MP2)//B3LYP theoretical level is expected to provide the energetic parameters with 'chemical accuracy' within 3-6 kJ mol$^{-1}$ in terms of average absolute deviations. The ab initio calculations were performed using the GAUSSIAN 09 and MOLPRO 2010 program packages.

Rate constants for various primary and secondary reactions involved in the pyrolysis were computed by solving the one-dimensional master equation employing the MESS package. Here, rate constants $k(T)$ for individual reaction steps were calculated within RRKM (unimolecular reactions) or transition state theory (TST, bimolecular reactions) generally utilizing the Rigid-Rotor, Harmonic-Oscillator (RRHO) model for the calculations of partition functions for molecular complexes and transition states. Collisional energy transfer rates in the master equation were expressed using the "exponential down" model, with the temperature dependence of the range parameter $\alpha$ for the deactivating wing of the energy transfer function expressed as

$\alpha(T) = \alpha_{300}(T/300\ \text{K})^n$, with $n = 0.86$ and $\alpha_{300} = 228\ \text{cm}^{-1}$ obtained earlier from classical trajectories calculations as ‘universal’ parameters for hydrocarbons in the nitrogen bath gas. We used the Lennard-Jones parameters ε and σ were derived based on the fit of results using the “one-dimensional optimization” method.

For *n*-decane, *n*-dodecane, and butylbenzene systems, the barrierless single-bond cleavage reactions were treated using phase space theory with the empirical potential energy parameters selected in such a way that the calculated rate constants for the reverse radical recombination reactions reproduced the rate constants for the prototype $C_2H_5$ + $C_2H_5$ and $C_2H_5$ + H and other appropriate reactions studied earlier by Klippenstein and co-workers using the most accurate up-to-date theoretical approach, variable reaction coordinated transition state theory (VRC-TST). Alternatively, in the study of JP-10 pyrolysis, we ourselves applied the VRC-TST approach for all barrierless decomposition pathways in the primary and secondary decomposition channels. In this case, the potential energy calculations were carried out using the multireference second-order perturbation theory CASPT2 method with the cc-pvdz basis set. This method is suitable for a computationally efficient treatment of the multi-reference character of the wave function for radical–radical reactions. Because of computational limitations, the minimal (2e,2o) active space was a default choice in the CASPT2 calculations, which is generally adequate for the description of static electronic correlation in a process of a single bond cleavage or a reverse process of bond formation from two radicals. A failure in an active space choice could be seen in an irregular character of the calculated minimal energy reaction path (MEP) on a PES for a radical-radical association. For instance, in the case of $C_2H_3$ + cyclopentenyl ($C_5H_7$) association – the reverse process for dissociation of 3-vinyl-1-cyclopentene, the calculations with a (2e,2o) active space resulted in a non-monotonic MEP. In this case, we assumed that all delocalized π orbitals of the $C_5H_7$ fragment are of importance and need to be included in the active space. In fact, one has to include the entire π system, which consists of 2 π electrons in the $C_2H_3$ fragment and 3 π electrons in the $C_5H_7$ fragment. Together with the unpaired electron in $C_2H_3$, this resulted in a (6e,6o) active space. The (6e,6o) active space proved to be adequate for the $C_2H_3$ + $C_5H_7$ association reaction as it produced a smooth and monotonic MEP.

The hindered rotor treatment was applied only to smaller $C_3H_7$ and $C_4H_9$ radicals while dealing with their $\beta$-scission reactions. For these species, soft normal modes were visually examined and those representing internal rotations were considered as one-dimensional hindered rotors in partition function calculations. For larger alkyl radicals, $C_5H_{11}$, $C_6H_{13}$, $C_7H_{15}$, $C_8H_{17}$, and $C_9H_{19}$, only terminal $CH_2$, $CH_3$, and $C_2H_4$ rotations were treated as hindered rotors, whereas all other convoluted rotations were treated as harmonic oscillators. One-dimensional torsional potentials were calculated by scanning PESs at the B3LYP/6-311G(d,p) level of theory. For comparison, we also performed calculations of the same rate constants in pure RRHO approximation and found that the replacement of harmonic oscillators with hindered rotors increases the $\beta$-scission rate constants by 8-41% at 1000 K, but the difference drops to only 2-25% at 1,600 K. For *n*-decane, *n*-dodecane and decyl and dodecyl radicals, visual identification of internal rotations is not practically possible because those are coupled with one another and with other types of motions. Therefore, these species were treated within RRHO keeping in mind the above mentioned error bars in rate constants. At the same time, the expected errors in ratios of rate constants are expected to be smaller than the errors in their absolute values due to cancelations of similar inaccuracies. Hence we anticipate that the relative product yields are predicted by our calculations with higher accuracy.

An implementation of the strategy described above and methods to study the complete pyrolysis mechanism of such large molecules as *n*-decane, *n*-dodecane, butylbenzenes, and JP-10 is a challenging task due to numerous decomposition pathways with a large number of possible isomers, transition states and bimolecular products. To overcome this problem we developed a software package, Pyrol, to automate the implementation of our strategy for computational studies of pyrolysis of hydrocarbon molecules. Starting with a closed-shell entity Pyrol first creates a map of all possible initial C-H bond cleavages. If there is a C-C bond cleavage which leads to a direct fragmentation, this channel can be added manually to the reaction map. Next, Pyrol generates input files for GAUSSIAN 09 and MOLPRO 2010 to calculate energies and molecular properties for the species of interest. After the calculations of the initial bond cleavages are finished, the software gathers the results and a decision whether some of the decomposition channels are too unfavorable and can be excluded can be made. Next, Pyrol analyzes all possible C-C $\beta$-scissions in the radicals produced by the initial C-H (C-C) bond cleavages and the decomposition map is updated accordingly. Again, there is a possibility to edit the map manually to remove or add some desirable channels, such as possibly favorable C-H $\beta$-scissions and H migrations. After the decomposition map is updated, the GAUSSIAN 09 and MOLPRO 2010 input scripts for $\beta$-scission routes are generated. This process is repeated recursively until a bond cleavage in each channel ends up with final bimolecular products considered to be stable under given conditions. The resulting PES and calculated molecular properties are than processed by the kinetics facility of Pyrol to generate input files for rate constant calculations by the MESS package. Finally, after the rate constants calculations by MESS are completed, Pyrol solves unimolecular kinetic equations using the steady state approximation to obtain temperature and pressure dependences for the overall decomposition rate constant and for the product branching ratio.

## Publications

P1: Zhao, L., et al., Combined experimental and computational study on the unimolecular decomposition of JP-8 jet fuel surrogates. I. *n*-Decane ($n$-$C_{10}H_{22}$). *J. Phys. Chem. A*, 121 (6), 1261-1280 (**2017**).

P2: Zhao, L., et al., Combined experimental and computational study on the unimolecular decomposition of JP-8 jet fuel surrogates. II: *n*-Dodecane ($n$-$C_{12}H_{26}$). *J. Phys. Chem. A*, 121 (6), 1281-1297 (**2017**).

P3: Zhao, L., et al., A vacuum ultraviolet photoionization study on high-temperature decomposition of JP-10 (*exo*-tetrahydrodicyclopentadiene). *Phys. Chem. Chem. Phys.*, 19 (24), 15780-15807 (**2017**).

P4: Belisario-Lara, D., et al., Computational study on the unimolecular decomposition of JP-8 Jet Fuel Surrogates III: Butylbenzene isomers (*n*-, *s*-, and $t$-$C_{14}H_{10}$). *J. Phys. Chem. A*, 122 (16), 3980–4001 (**2018).**

P5: Morozov, A. N., et al., A theoretical study of pyrolysis of exo-tetrahydrodicyclopentadiene and its primary and secondary unimolecular decomposition products. *J. Phys. Chem. A*,, 122 (22), 4920–4934 (**2018**).